Altering lipid A precursor ion-types in the gas phase for in-depth structural elucidation via tandem mass spectrometry

Hsi-Chun Chao[1,†] and Scott A. McLuckey[1,*]

[1]Department of Chemistry, Purdue University, Indiana, 47907
[†]Beckman Institute for Advanced Science and Technology, University of Illinois Urbana-Champaign, Illinois, 61801

*Address correspondence to:
Dr. Scott A. McLuckey
560 Oval Drive
Department of Chemistry
Purdue University
West Lafayette, IN 47907-2084, USA
Phone: (765) 494-5270
Fax: (765) 494-0239
E-mail: mcluckey@purdue.edu

Abstract

Lipid A, a well-known saccharolipid, acts as the inner lipid-glycan anchor of lipopolysaccharides in Gram-negative bacterial cell membranes and functions as an endotoxin. Its structure is comprised of two glucosamines with β(1→6) linkages and various fatty acyl and phosphate groups. Lipid A structure can be used for identification, but its complexity poses significant structural characterization challenges. In this work, we present a comprehensive strategy combining condensed phase sample preparation, electrospray ionization, and gas-phase ion/ion reactions with tandem mass spectrometry for detailed lipid A structural elucidation. We use proton transfer reactions, charge-inversion reactions, and sequential ion/ion reactions for magnesium transfer to generate targeted lipid A ions. The strategy, established with a synthetic monophosphoryl lipid A (MPLA) and known MPLA and diphosphorylated lipid A (DPLA) from *E. coli* F583, demonstrated that $[MPLA-2H]^{2-}$, $[MPLA-H]^{-}$, and $[MPLA-H+Mg]^{+}$ precursor ions offer complementary information for MPLA, while $[DPLA-H]^{-}$, $[DPLA+H]^{+}$, and $[DPLA-H+Mg]^{+}$ precursor ions provide analogous information for DPLA analysis. We validated the strategy using known lipid A species and also successfully applied this strategy to profile unknown MPLA and DPLA in the same *E. coli* strain.

Introduction

Saccharolipids (SLs) constitute a lipid subclass that is comprised of both glycan and lipid structural components.[1] In contrast with glycolipids, wherein a glycan is linked to a sphingolipid backbone via a glycosidic bond, saccharolipids feature fatty acyl components that are directly linked to sugars.[2] Among the most widely known SLs is lipid A, which is the inner lipid-glycan anchor region of lipopolysaccharides (LPS) relevant to cell membranes in Gram-negative bacteria. The general lipid A structure contains two glucosamines with β(1→6) linkages and various fatty acyl groups and phosphate groups bound to the different sites on the sugar (**Figure 1**.) Lipid A is an endotoxin from gram-negative bacteria that triggers a pathogenic immune response in the host (e.g., human), which can lead to severe health conditions, such as septic shock.[3-4] The endotoxin is species-specific, suggesting that lipid A can be useful for identifying bacterial species as well as understanding the bioactivity of the endotoxin.[5-7] Moreover, it can be a potential target for antibiotic discovery. However, the complexity of the structure makes the characterization of lipid A extremely challenging, which is a complicating factor in profiling lipid A from bacterial samples. Therefore, an analytical strategy capable of generating extensive structural information from lipid A is an emerging need.

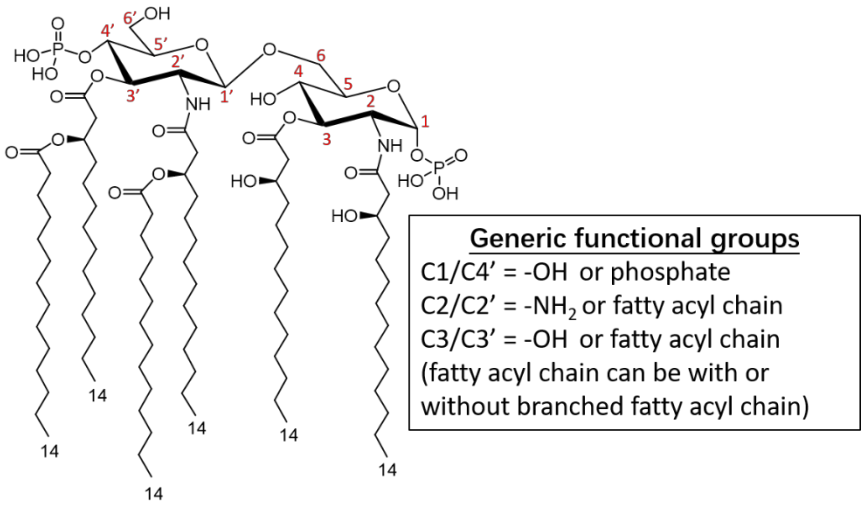

Figure 1. The generic structure of diphosphoryl lipid A (DPLA-1825.) The phosphorylation sites are either on the C1 or C4' position for mono-phosporyl lipid A (MPLA), or both for DPLA. The different fatty acyl substitutents could be on C2/C3/C2'/C3' position with the potential for an O-linked fatty acyl branch. The fatty acyl chains that are directly esterified to the sugar are primary fatty acyl chains, and the O-linked branch fatty acyl chains are secondary fatty acyl chains.

Several lipid A species from various origins, including *E. coli* and *C. trachomatis*, and their respective variants, were identified by leveraging biological and chemical knowledge.[8-9] The confirmation usually came from complementary information derived from nuclear magnetic resonance spectroscopy (NMR) and mass spectrometry (MS) for the sugar linkage and fatty acyl contents, respectively.[10] Although NMR is a powerful tool for structural elucidation, the sensitivity of NMR remains an issue for profiling trace species in biological samples. On the other hand, MS is often capable of profiling low abundance molecules in complex sample matrices. In the case of lipid A, matrix-assisted laser desorption/ionization (MALDI) combined with MS has been the most commonly used approach for lipid A analysis for decades.[11-12] Lipid A ions can be generated via MALDI in either the negative or positive ion mode, depending on the matrix, and the resulting lipid A ions are usually either $[M-H]^-$ in the negative mode or $[M+Na]^+$ in the positive mode.[13-14] To elucidate ion structure, tandem MS (MS/MS) is commonly employed, and collision-induced dissociation (CID) is the most extensively used dissociation technique, in part due to its widespread availability. MALDI-MS/MS using CID, primarily on quadrupole/time-of-flight (Q/TOF) or TOF/TOF platforms, has been used to characterize lipid A structures.[15-17] However, extensive structural characterization of a given lipid A by MS^2 alone is challenging due to the diversity of structures that may be present. Therefore, Park et al. reported the coupling of a quadrupole ion trap (QIT) with a TOF analyzer, thereby enabling MALDI-MS^n experiments for characterizing lipid A structures.[18] Electrospray ionization (ESI), which is readily interfaced with condensed-phase separation techniques as well as MS^n platforms, has also been applied to the characterization of lipid A from biological matrices.[19-23] In addition to CID, alternative dissociation approaches,

such as infrared multiphoton dissociation (IRMPD)[24-25] and ultraviolet photodissociation (UVPD),[26-27] have been explored for elucidating lipid A structures. Each dissociation method has relative strengths and weaknesses. For example, ESI-MS^n experiments with CID or IRMPD usually require multistage dissociation to reveal a comprehensive map of lipid A structure because MS^2 usually provides only the length of the fatty acyl groups but no cross-ring fragmentation from the glycan. In contrast, UVPD is able to generate cross-ring fragmentation, but the tuning efficiency (abundance of fragment ions) is relatively low and requires novel instrumentation for low signal-to-noise detection for those fragment ions.[7, 26-28]

The use of different dissociation methods can often provide complementary structural information from a given ion-type. However, it is also often of benefit to probe different ion-types generated from the same molecule.[29] To this end, Aissa et al. proposed a lipid A structural characterization strategy that subjects different lipid A cation-types to CID to provide complementary structural information via ESI-MS^n. It was shown that sodiated and di-sodiated lipid A cations ($[M+Na]^+$ and $[M-H+2Na]^+$) can provide in-depth acyl linkage information at the C3' secondary (branched) and C3/C3' primary positions.[30] Combined with information from previous reports that protonated molecules ($[M+H]^+$) or triethylammonium adducts ($[M+Et_3N]^+$) would generate an oxonium ion upon CID, which was assigned as the distal sugar fragment,[31-32] both acyl linkage and phosphorylation site could be determined from the various precursor ion-types.

In both MALDI and ESI, the predominant ion-types are influenced strongly by sample preparation conditions (i.e., matrix[33] or solution[34] conditions), which can limit the available ion-types for subsequent tandem MS analysis. It is therefore desirable to generate different ion-types efficiently and rapidly from the most abundant ion-type generated from the ionization process. It has been shown in multiple analytical contexts[35] that gas-phase ion/ion reactions can be used to alter ion-types quickly and efficiently within the mass spectrometer. Recently, our group developed a series of ion/ion reaction approaches for ion-type transformation

relevant to the structural characterization of various lipid types, including fatty acids,[36-37] glycerophospholipids, [38-39] cardiolipins,[40-41] and various sugar-lipid conjugates, including glycolipids[42-43] and phosphoinositides.[44] We also established a workflow that combines several different ion/ion reactions, including proton transfer, metal ion transfer, and charge inversion, to generate targeted ion-types for comprehensive glycan coverage of different subtypes of gangliosides.[45] In this work, we implemented a variety of gas-phase ion/ion reactions to produce different ion-types from lipid A for structural characterization. Both synthetic and known biological lipid A species were used to explore ion-types generated via ion/ion reactions to develop a strategy for extensive lipid A structural characterization. The strategy was then applied for the characterization of unknown lipid A species from *E. coli* extracts.

Experimental Section

Materials. Synthetic monophosphoryl lipid A (MPLA-PHAD®) was purchased from Avanti Polar Lipids, Inc. (Alabaster, AL). Monophosphoryl and diphosphoryl lipid A extract from *E. coli* F583 (Rd mutant), magnesium chloride ($MgCl_2$), 2,2';6',2"-terpyridine (Terpy), and proton sponge (N, N, N′, N′-tetramethyl-1,8-naphthalenediamine, PrS) were purchased from Sigma-Aldrich (St. Louis, MO). MS-grade methanol (MeOH), LC-grade chloroform ($CHCl_3$), polyethylenimine-4k (PEI-4k) and ammonium hydroxide (28% to 30% NH_4OH solution) were purchased from Fisher Scientific (Pittsburgh, PA).

Sample Preparation. Stock solutions of lipid A and extracts (porcine brain) were prepared in MeOH/$CHCl_3$ (v/v, 50/50) to a concentration of 0.5 or 1 mg-mL^{-1}, and stored at −80 °C. Before the analysis, the stock solutions were diluted using MeOH to 0.01 mg-mL^{-1}. An aliquot of NH_4OH solution was spiked into the sample solution to make the sample with ~0.1% (v/v) NH_4OH solution (basic condition.) For metal-ligand complex reagents (e.g. $[Mg(Terpy)_2]^{2+}$), $MgCl_2$ and Terpy were mixed in MeOH with 1:1 (molar ratio) to a final concentration of ~50

μM. Proton sponge powder was dissolved in MeOH with the stock concentration at 1 mM, and then spiked into the metal-Terpy complex solution with a final concentration of 20 μM.

Mass Spectrometry. All experiments were performed on a TripleTOF 5600 quadrupole time-of-flight mass spectrometer (SCIEX, Concord, ON, Canada) that has been modified for ion/ion reactions.[46] Alternately pulsed dual nano-electrospray ionization (nESI) allows for the sequential injection of anions and cations.[47] Doubly deprotonated lipid A ions (e.g., $[MPLA-2H]^{2-}$ or $[DPLA-2H]^{2-}$) were generated directly from ESI. Singly deprotonated species were generated via a gas-phase proton transfer reaction. Doubly deprotonated lipid A ions and proton sponge cations ($[PrS+H]^+$) were alternately generated via nESI, mass-selected in Q1, and transferred to q2 for mutual storage (10-30 ms) to produce singly deprotonated lipid A ions ($[MPLA-H]^-$ or $[DPLA-H]^-$). A supplemental AC voltage at the secular frequency of the targeted proton transfer product was applied during the entire mutual storage period to inhibit complete neutralization of the anion by ion parking.[48] For charge-inversion to produce $[MPLA+H]^+$ and $[DPLA+H]^+$ cations from doubly-deprotonated anions, a variation of a previously described process for charge inverting cations to anions was used.[49] Specifically, a mixture of multiply-charged PEI cluster cations was selected and reacted with a doubly deprotonated lipid A anion, thereby resulting in the formation of a singly protonated lipid A species. For the generation of ($[MPLA-H+Mg]^+$ or $[DPLA-H+Mg]^+$) cations, sequential ion/ion reactions were performed. First, doubly deprotonated lipid A ions were generated via nESI, and stored in q2. Next, both $[PrS+H]^+$ and metal-ligand complex ($[Mg(Terpy)_2]^{2+}$) ions were generated via alternately pulsed nESI, but only $[PrS+H]^+$ was mass-selected in Q1 and transferred to q2 for mutual storage (10-30 ms). Sequential resonance ejection ramps[50] were used to mass-select targeted singly deprotonated ions for subsequent reaction. Another pulse from the cation emitter was applied and $[Mg(Terpy)_2]^{2+}$ was mass-selected and transferred to q2 for mutual storage (10-30 ms). Further sequential resonance ejection ramps in q2 were used

to mass-select targeted ion/ion reaction product ions for MS^n experiments via ion-trap CID and mass analysis via TOF.

Results and Discussion

Lipid A signal enhancement via condensed-phase pH adjustment. Lipid A structures generally consist of two glucosamine (amino-sugar) units, in a β (1→6) linkage, with one phosphate at either the C1 or C4' position, in the case of mono-phosphoryl lipid A (MPLA), or at both the C1 and C4' positions, in the case of di-phosphoryl lipid A (DPLA) (see **Figure 1**).[51] It is therefore common to use ESI in the negative mode for the analysis of lipid A due to the ease of deprotonation. During the analysis of synthetic MPLA, we observed both the 1− and 2− charge states under the normal solution conditions (i.e., samples dissolved in mostly methanol) (**Figure S1**), with the former being most prominent. The presence of the 2− ion suggests the potential deprotonation at the phosphate group and one of the hydroxy groups. Under similar solution conditions, complicated spectra were observed from the analysis of MPLA extracts from *E. coli* samples (**Figure 2a**), leading to relatively low ion signals for the precursor ions (either $[MPLA-H]^-$ or $[MPLA-2H]^{2-}$). Therefore, to enhance the MPLA ion signals for further tandem mass spectrometry analysis, we modified the sample solution by adding ~0.1% NH_4OH, leading to a roughly 15-fold MPLA signal enhancement with most of the signal arising from doubly deprotonated species ($[MPLA-2H]^{2-}$ (**Figure 2b**)). The same strategy was also applied to DPLA-containing samples with similar signal enhancements for the DPLA species (data not shown).

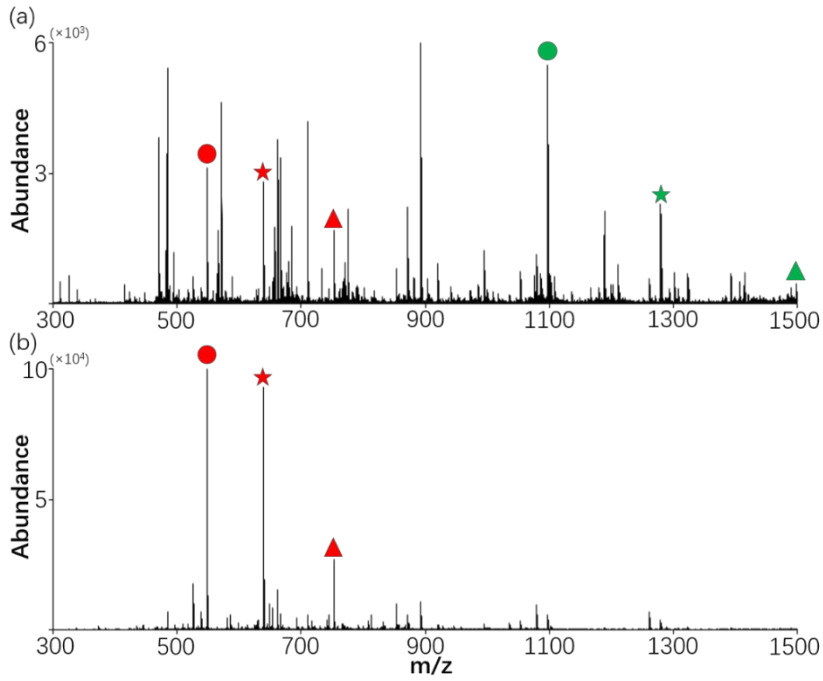

Figure 2. Optimization of sample solution to enhance precursor ion signals. (a) MeOH and (b) 0.3% NH_4OH in MeOH. The concentration of the two solution are the same at ~1mg mL^{-1} of the *E. coli* extract. The circle symbol (●) represents MPLA-1099, the star symbol (★) represents MPLA-1287, and the triangle (▲) represents MPLA-1507. The green colored symbols are the signals from 1− charge state, and the red colored symbols are the signals from 2− charge state of the MPLAs.

The analysis of MPLA via gas-phase chemistry. The most abundant ion-type generated via negative nESI in this work, $[MPLA-2H]^{2-}$, was probed by ion trap CID and used as the precursor ion in various ion/ion reactions to generate other ion-types for subsequent ion trap CID. Other ion types, including singly deprotonated MPLA ($[MPLA-H]^-$), protonated MPLA ($[MPLA+H]^+$), and magnesium-transferred MPLA ($[MPLA-H+Mg]^+$) were also investigated. The reactions for generating these targeted ion types and the respective tandem mass spectra (after ion-trap CID) are provided in the following text. First, we summarize the key information obtained from each ion type. CID of $[MPLA-2H]^{2-}$ reveals the profile of fatty acyl groups on lipid A through both neutral loss and complementary fatty acyl-related fragment ions. Similarly, $[MPLA-H]^-$ offers comparable information but does not provide additional structural insights. $[MPLA+H]^+$ yields significant structural information from the cleavage of the glycosidic bond. Lastly, the magnesium-transferred ion reveals the fatty acyl chain location

relative to the proposed magnesium-phosphate coordination site, allowing for the identification of fatty acyl compositions on the lipid A structure. In the following sections, we use both synthetic lipid A, synthetic MPLA (PHAD®), and biological lipid A from the *E. coli* F583 strain to detail our findings.

First, the doubly charged synthetic MPLA (PHAD®) ($[MPLA\text{-}PHAD®-2H]^{2-}$, *m/z* 871.6) was subjected to ion trap CID, and the spectrum is shown in **Figure 3a**. The dominant fragments (labeled 2 and 2' in **Figure 3a**) arise from cleavage of the ester linkage on the C3 position leading to the loss of C14:0 (3-OH) (*m/z* 1500.1, fragment 2) and its complementary deprotonated fatty acid (*m/z* 243.2, fragment 2'). Two other complementary fragment ion pairs are also observed, including *m/z* 1516.1 and *m/z* 227.2 (fragment 1 and 1'), arising from loss of a C14:0 fatty acid from either the C2' or C3' carbons; and *m/z* 1459.1 and *m/z* 284.2 (fragment 3 and 3'), suggesting the in-ring fragment ions of $^{0,2}X_0$ and $^{0,2}A_2$, respectively.

The singly-deprotonated species was then generated from the doubly-deprotonated ion via gas-phase proton transfer to determine if complementary structural information might be obtained via CID. **Figure S2** demonstrates the proton transfer reaction between the proton sponge cation and $[MPLA-2H]^{2-}$. The results suggested no or minimal ion loss from the isolation of the precursor and proton transfer reaction. After the proton transfer reaction, $[MPLA\text{-}PHAD®-H]^{-}$ (*m/z* 1744) was subjected to ion trap CID, and the results are shown in **Figure 3b**. The dominant 228 Da loss (*m/z* 1516.1, fragment 1) and 244 Da loss (*m/z* 1500.1, fragment 3) arise from the ester bond cleavages also observed with the doubly deprotonated MPLA (i.e., loss of a C14:0 fatty acid and a loss of a C14:0 (3-OH) fatty acid, respectively). A pair of minor fragment ions arising from 436 Da loss (*m/z* 1308, fragment 4) and 454 Da loss (*m/z* 1290, fragment 5) are consistent with cleavages on either side of the oxygen bound to the C3' carbon (i.e., fatty acid loss (454 Da) and ketene loss (436 Da). A fragment ion corresponding to 472 Da loss is consistent with the combination of losing a C14:0 fatty acid branch (228 Da) and the C14:0(3-OH) fatty acid (244 Da) (*m/z* 1272, fragment 6). However,

no significant additional information was observed from this ion-type.

Next, we generated the singly protonated analyte via charge inversion of the doubly deprotonated MPLA. We used multiply charged protonated PEI ions arising from PEI-4k ($[PEI\text{-}4k+nH]^{n+}$) for the reaction. Briefly, $[MPLA-2H]^{2-}$ ions were generated, mass-selected, transferred, and stored in q2 (**Figure S3a**). PEI cations were then generated via positive nESI, and a wide range of PEI cations (**Figure S3b**) for the reaction was mass-selected and transferred into q2. The post-reaction spectrum is shown in **Figure S3c**. We further mass-selected and subjected the $[MPLA\text{-}PHAD®+H]^{+}$ ion (*m/z* 1746.3) to ion trap CID. The result shows a dominant B_1 fragment ion at *m/z* 1114.8 (fragment 7), consistent with the literature[1], suggesting the cleavage of the glycosidic linkage (**Figure 3c**). This structural information is useful for determining the two different amino sugar-fatty acid conjugates units, where the synthetic MPLA-PHAD shows the phosphorylation site to be exclusively on the C4' position. Therefore, this ion can potentially indicate the phosphorylation site. The losses of one and two water molecules are also observed along with a minor signal that is consistent with the loss of a C14:0 fatty acid (228 Da loss). We isolated the B_1 ion for another round of ion trap CID and the result shows a dominant loss in 228 Da, suggesting the C14:0 fatty acid is on the first amino sugar-fatty acid conjugate unit (**Figure S4**). The secondary fragment ion with 454 Da loss (*m/z* 660) is also observed, suggesting the loss of entire C3' fatty acid unit. Moreover, a 552 Da loss (*m/z* 562) was also observed, which is the combined loss of phosphate (98 Da) and C3' fatty acid unit (454 Da.).

As a final ion-type examined here, we generated magnesium ion-containing species via a sequential ion/ion reaction process.[44-45] The precursor ion, $[MPLA\text{-}PHAD®-2H]^{2-}$, was reacted with protonated proton sponge ($[PrS+H]^{+}$) to produce the singly deprotonated anion, $[MPLA\text{-}PHAD®-H]^{-}$. The deprotonated species was then subjected to another ion/ion reaction with $[Mg(Terpy)_2]^{2+}$, which generated the complex species $[MPLA\text{-}PHAD®-H+Mg(Terpy)]^{+}$. The latter species is generated from the attachment of the reactant ions to one another with the

spontaneous loss of one Terpy ligand. An additional step of CID of [MPLA-PHAD®−H+Mg(Terpy)]$^+$ leads to the loss of the second Terpy ligand, thereby generating the [MPLA-PHAD®−H+Mg]$^+$ ion (*m/z* 1768.3). Ion trap CID of the latter ion (**Figure 3d**) is dominated by the neutral losses of 228 Da (i.e., loss of a C14:0 fatty acid) and 454 Da (i.e., loss of the group bound to C3' as a fatty acid).

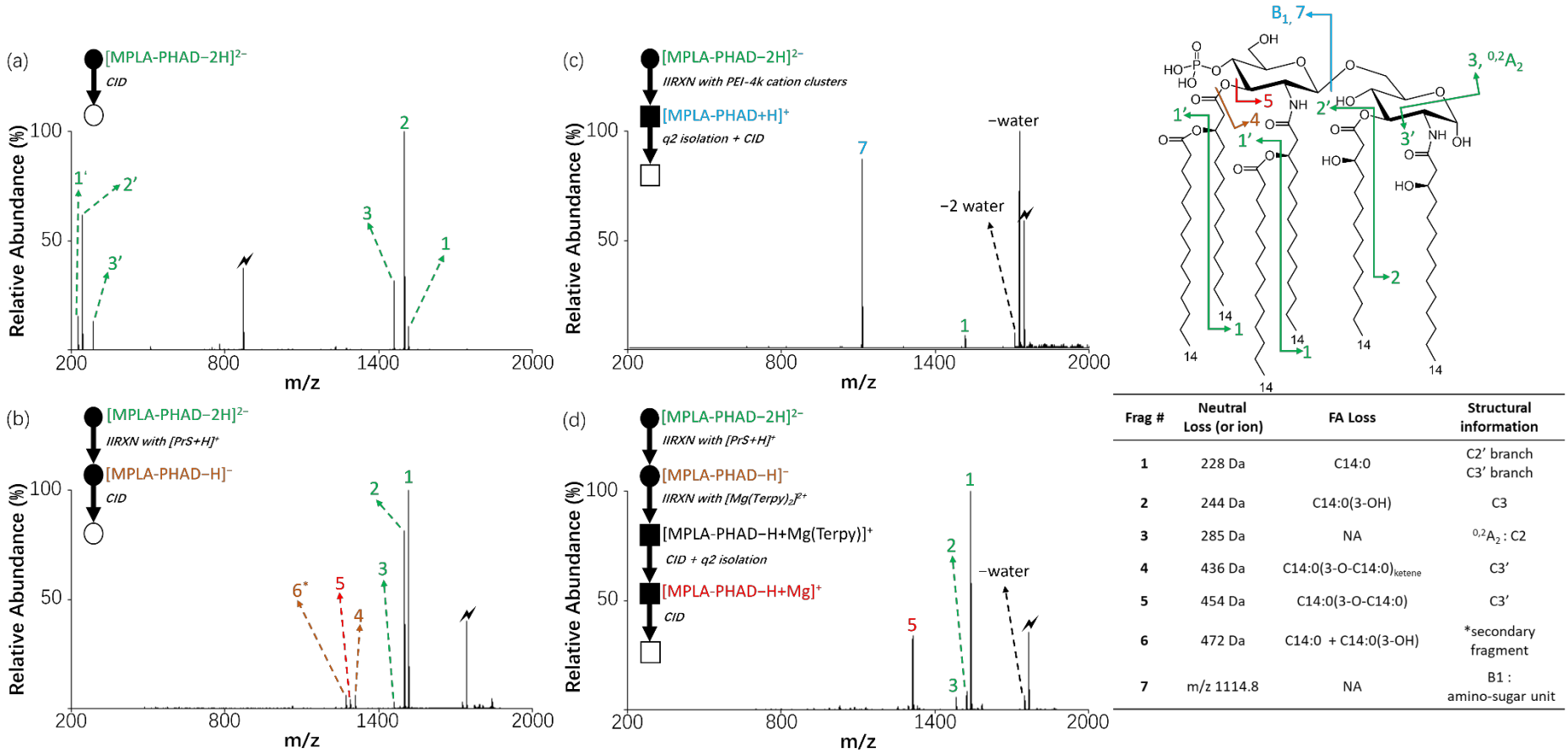

Frag #	Neutral Loss (or ion)	FA Loss	Structural information
1	228 Da	C14:0	C2′ branch C3′ branch
2	244 Da	C14:0(3-OH)	C3
3	285 Da	NA	$^{0,2}A_2$: C2
4	436 Da	C14:0(3-O-C14:0)$_{ketene}$	C3′
5	454 Da	C14:0(3-O-C14:0)	C3′
6	472 Da	C14:0 + C14:0(3-OH)	*secondary fragment
7	m/z 1114.8	NA	B1 : amino-sugar unit

Figure 3. The CID mass spectra of different MPLA-PHDA ions, (a) [MPLA-PHAD®−2H]$^{2-}$, *m/z* 817.6, (b) [MPLA-PHAD®−H]$^{-}$, *m/z* 1744.3, (c) [MPLA-PHAD®+H]$^{+}$, *m/z* 1746.3, and (d) [MPLA-PHAD®−H+Mg]$^{+}$, *m/z* 1768.3.

The same ion types described above from the synthetic MPLA-PHAD® were also examined for the three major MPLA ions generated from the MPLA extract from *E. coli* F583 observed at *m/z* 548.3 (2−), *m/z* 639.4 (2−), and *m/z* 752.5 (2−) (**Figure 2b**). The structure of the 1507 Da MPLA, referred to here as MPLA-1507, in the *E. coli* F583 sample, as reflected by the dianion at *m/z* 752.3, has previously been elucidated/proposed[27] (see structure in **Figure 4**). **Figure 4** shows the CID spectra from different ion-types of MPLA-1507 including $[\text{MPLA-1507}-2\text{H}]^{2-}$, $[\text{MPLA-1507}-\text{H}]^{-}$, $[\text{MPLA-1507}+\text{H}]^{+}$, and $[\text{MPLA-1507}-\text{H}+\text{Mg}]^{+}$. The results are consistent with those observed with the synthetic MPLA-PHAD ions. For example, fatty acyl chain information is obtained from the doubly deprotonated species (**Figure 4a**), including a 200 Da loss (*m/z* 1305.8 and complementary ion at *m/z* 199.2, fragment 1 and 1') corresponding to a C12:0 fatty acid, a 244 Da loss (*m/z* 1261.8 and the complementary ion at *m/z* 243.2, fragments 2 and 2') from the loss of a C14:0(3-OH) fatty acid, and a 285 Da loss (*m/z* 1220.8 and the complementary ion at *m/z* 284.2 from the inner-ring fragmentation, fragments 3 and 3'). The loss of a C14:0(3-OH) fatty acid can arise from the C3 and/or C3' positions. The C12:0 fatty acid loss arises from the C3' branch and the 285 Da loss indicates the inner-ring cleavages $^{0,2}X_0$ and $^{0,2}A_2$, respectively.

The ion trap CID product ion spectrum of the singly deprotonated precursor anion ($[\text{MPLA-1507}-\text{H}]^{-}$, *m/z* 1506.0, **Figure 4b**) is dominated by the loss of 244 Da (i.e., C14:0(3-OH) fatty acid loss from the C3 and/or C3' sites). Other fragment ions of lower relative abundance were observed including water loss, 182 Da loss (*m/z* 1323.9, fragment 4), nominal ketene loss for C2 branch (C12:0), 226 Da loss (*m/z* 1279.8, fragment 5), which can occur from nominal ketene loss from C3 and/or C3' sites or from amide bond cleavage at C2, 285 Da loss (*m/z* 1220.8, fragment 3), which is also observed with the dianion (see **Figure 4a**) and 408 Da loss (*m/z* 1097.7, fragment 5). The latter ion can arise from a combined loss of 226 Da (nominal ketene loss from the C3, C3', or C2 sites) and 182 Da (nominal ketene loss from the C2' branch site) or as a single step via amide bond cleavage at C2' giving rise to nominal ketene loss of

the fatty acyl chains attached to the amide nitrogen.

CID of protonated MPLA-1507 ($[MPLA\text{-}1507+H]^+$, **Figure 4c**), generated via charge inversion, shows dominant cleavage of the glycosidic bond with charge retention on the B_1 fragment (*m/z* 876.5, fragment 6). Smaller peaks reflect losses of 200 Da (*m/z* 1308, fragment 1) and 244 Da (*m/z* 1264, fragment 2) reflecting ester bond cleavages that are also observed with the singly deprotonated species (**Figure 4a**). With further CID of the *m/z* 876 ion (**Figure S5**), 182 Da loss (*m/z* 694, C12:0 ketene loss) and 200 Da loss (*m/z* 676, C12:O fatty acid loss) confirmed that the C12:0 branch is on the first amino-sugar unit. A prominent loss of 408 Da is also observed, which can arise from a combined loss of 226 Da (nominal ketene loss from the C3' site) and 182 Da (nominal ketene loss from the C2' branch site) or as a single step via amide bond cleavage at C2' giving rise to nominal ketene loss of the fatty acyl chains attached to the amide nitrogen. A relatively modest signal arising from a loss of 342 Da is also noted, which is consistent with the loss of phosphate (98 Da) and the C3' fatty acid (244 Da), indicating C4' phosphorylation in the general structure of lipid A (**Figure 1**). According to the literature, if a mixture of isomeric MPLA with either C1 or C4' phosphorylation were present, two B1 ions with a 80 Da difference would be observed.[22, 30] In this case, no C1 phosphorylation was detected.

Figure 4d shows the CID spectrum of $[MPLA\text{-}1507-H+Mg]^+$, the fourth ion-type examined for this molecule. It is noticed that slightly more information can be obtained from the Mg-transferred precursor comparing to singly deprotonated species. A dominant 244 Da loss (*m/z* 1285.8, fragment 2) is observed, which is similar to the CID results for $[MPLA\text{-}1507-H]^-$. However, assuming $[MPLA\text{-}1507-H+Mg]^+$ to fragment similarly to $[MPLA\text{-}PHAD®-H+Mg]^+$ (see **Figure 3d**), the ester cleavage at the C3' position might be expected to be favored over the ester cleavage at the C3 position (compare, for example, fragment 5 to fragment 2 in **Figure 3d**). If this tendency holds for CID of $[Lipid\ A\text{-}H+Mg]^+$ in general, the 244 Da loss in **Figure 4d** would be expected to arise more from the C3' position than the C3

position. In addition to water loss, 184 Da loss (*m/z* 1345.8, fragment 7), 200 Da loss (*m/z* 1329.9, fragment 1), 226 Da loss (*m/z* 1303.8, fragment 4), and 285 Da loss (*m/z* 1244.8, fragment 3), are also observed suggesting the loss of branch C2' C12:0 fatty acid (aldehyde loss), branch C2' C12:0 fatty acid loss, cleavage at C3 or C3', and the C1-C2 inner-ring cleavage, respectively. Other secondary fragmentations, including 428 Da loss (*m/z* 1101.6), 444 Da loss (*m/z* 1085.7), and 529 Da loss (*m/z* 1001.6), can also be observed. These fragmentations likely result from combined losses such as 244 Da and 184 Da for the 428 Da loss, suggesting that the 184 Da loss may originate from the C2' branch or C2 or C3 cleavage; 244 Da and 200 Da for the 444 Da loss, likely involving the C3' and C2' branches at different cleavage sites; and 244 Da and 285 Da for the 529 Da loss, corresponding to a C3' and C1-C2 inner-ring cleavage.

After reviewing the results from the CID experiments, we can identify the information derived from each precursor ion type: (a) doubly deprotonated MPLA anions provide a general fatty acyl chain profile and potential C3 fatty acyl information; (b) protonated MPLA cations reveal information about the phosphorylation site through glycosidic bond cleavage (B1 ion) and fatty acyl positions on the sub amino-sugar unit; and (c) singly deprotonated MPLA anions and magnesium-transferred MPLA cations yield similar fragment profiles, but the magnesium-transferred cation offers better confidence in assigning C3' fatty acyl loss. Consequently, future analyses of MPLA should focus on the three key ion types: $[MPLA-2H]^{2-}$, $[MPLA+H]^{+}$, and $[MPLA-H+Mg]^{+}$. MPLA-1281, identified in the extracts and analyzed in a previous report,[27] was used to further test our strategy, and the three key ion types mentioned above gave spectra that are fully consistent with the previously proposed structure (**Figure S6**).

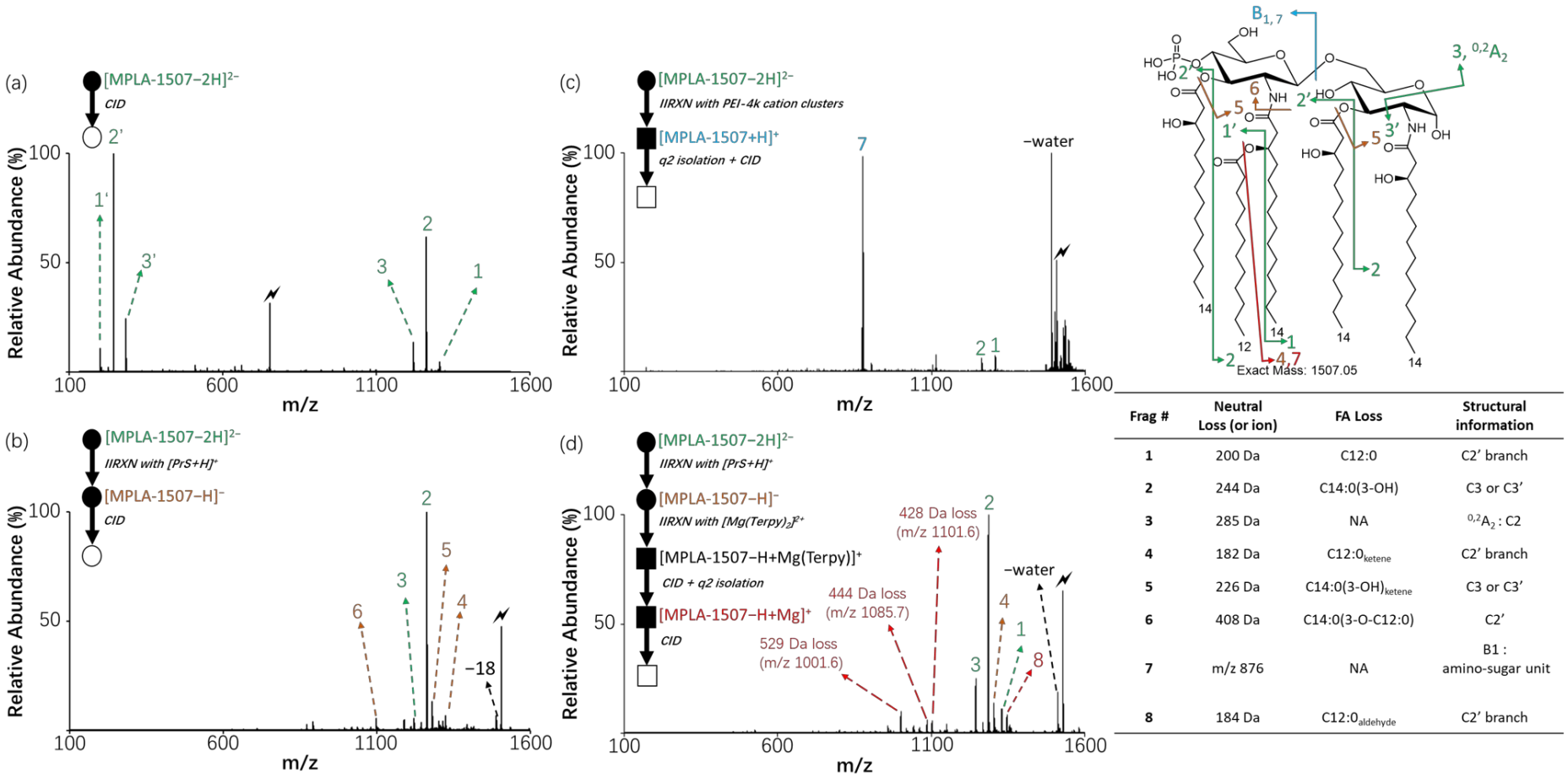

Frag #	Neutral Loss (or ion)	FA Loss	Structural information
1	200 Da	C12:0	C2′ branch
2	244 Da	C14:0(3-OH)	C3 or C3′
3	285 Da	NA	$^{0,2}A_2$: C2
4	182 Da	$C12:0_{ketene}$	C2′ branch
5	226 Da	$C14:0(3\text{-}OH)_{ketene}$	C3 or C3′
6	408 Da	C14:0(3-O-C12:0)	C2′
7	m/z 876	NA	B1 : amino-sugar unit
8	184 Da	$C12:0_{aldehyde}$	C2′ branch

Figure 4. The CID mass spectra of different MPLA-1507 ions, (a) $[MPLA\text{-}1507{-}2H]^{2-}$, *m/z* 752.5 (b) $[MPLA\text{-}1507{-}H]^{-}$, *m/z* 1506, (c) $[MPLA\text{-}1507{+}H]^{+}$, *m/z* 1508, and (d) $[MPLA\text{-}1507{-}H{+}Mg]^{+}$, *m/z* 1530.

Structural elucidation of unknown MPLA in E. coli F583 extract. In addition to MPLA-1507 and MPLA-1281, another major lipid A (*m/z* 548.3 (2−), **Figure 2b**), which is referred to here as MPLA-1099, was also profiled. We are unaware that the structure of this species has been described in the literature. Therefore, we used this unknown lipid A to test our MPLA structural elucidation strategy. $[MPLA\text{-}1099-2H]^{2-}$, $[MPLA\text{-}1099+H]^{+}$, and $[MPLA\text{-}1099-H+Mg]^{+}$ were produced via nESI and gas-phase ion/ion reactions and subjected to CID for the analysis of the structure. First, **Figure 5a** shows several fragments from the CID of $[MPLA\text{-}1099-2H]^{2-}$ (*m/z* 1097.7), including 226 Da loss (*m/z* 871.5, fragment 1), 244 Da loss (*m/z* 853.5, fragment 2), and 285 Da loss (*m/z* 812.5, fragment 3), where 226 Da and 244 Da losses suggest the presence of C14:0(3-OH). However, the base fragment peak corresponds to the 285 Da loss (fragment 3), which is likely the $^{0,2}A_2$ fragment, resulting from the loss of the C2-amide-bonded C14:0(3-OH) by C1-C2 inner-ring cleavage (**Figure 5a.**) This observation also suggests there may not be a fatty acyl group on either the C3 or C3' positions. This hypothesis is further supported by comparing the spectra in **Figures 3a** and **4a**, where a dominant 244 Da loss is observed, potentially corresponding to the loss of a hydroxy fatty acid (e.g., C14:0(3-OH) fatty acid).

Next, CID of $[MPLA\text{-}1099+H]^{+}$ (**Figure 5b**) shows the B1 ion at *m/z* 694, representing the first amino-sugar unit, fragment 4. This finding suggests that the second amino-sugar unit has a mass of only 405 Da, indicating the absence of a C3 fatty acyl chain. The observed loss of 285 Da results from the inner-ring cleavage of the C1-C2 unit, leaving no significant mass for an additional fatty acyl group on the second amino-sugar unit. Consequently, we propose that the second unit contains only a C2-amide-bonded C14:0(3-OH).

Finally, CID of $[MPLA\text{-}1099-H+Mg]^{+}$ shows a dominant 244 Da loss (fragment 2) which suggests a C14:0(3-OH) group on the C3' position, based on the fragmentation patterns from the previous $[MPLA-H+Mg]^{+}$ examples (**Figure 5c** compared to **Figure 3d** and **4d**). Also, a significant 60 Da loss (*m/z* 1061.7, fragment 5) was observed, which is a common $C_2H_4O_2$ loss

from inner-ring cleavage of hexose, suggesting the $^{3,4}A_2$ fragment, which is consistent with our hypothesis about the second amino-sugar unit (C3 with hydroxyl group). A minor 226 Da loss is also observed, which can be the nominal ketene loss of C14:0(3-OH) on C3' or on C2' via amide bond cleavage from the first glucosamine. This is consistent with other primary fragments, including 244 Da loss (fragment 2) and 285 Da (fragment 1), which suggest the fatty acyl chains on C3' and C2 positions, respectively. Other secondary fragment ions, including 304 Da loss (244 Da loss + 60 Da loss) and 346 Da loss (285 Da loss + 60 Da loss), were assigned respectively in the inserted structures. We also obtained the CID mass spectrum of the *m/z* 694 ion to check the secondary fragments obtained from **Figure 5b**. The result again validates our finding of C14:0(3-OH) at C3', where 342 Da loss (*m/z* 352 is consistent with phosphate 98 Da at C4' + 244 Da loss at C3') was observed. Also, a 184 Da loss is observed (*m/z* 510), which can be the cleavage of both C2' or C3', and 226 Da loss (*m/z* 468), which is the C3' or C2' cleavage (**Figure S7**). This example demonstrates the utility of probing complementary ion-types for in-depth structural elucidation of unknown MPLA species.

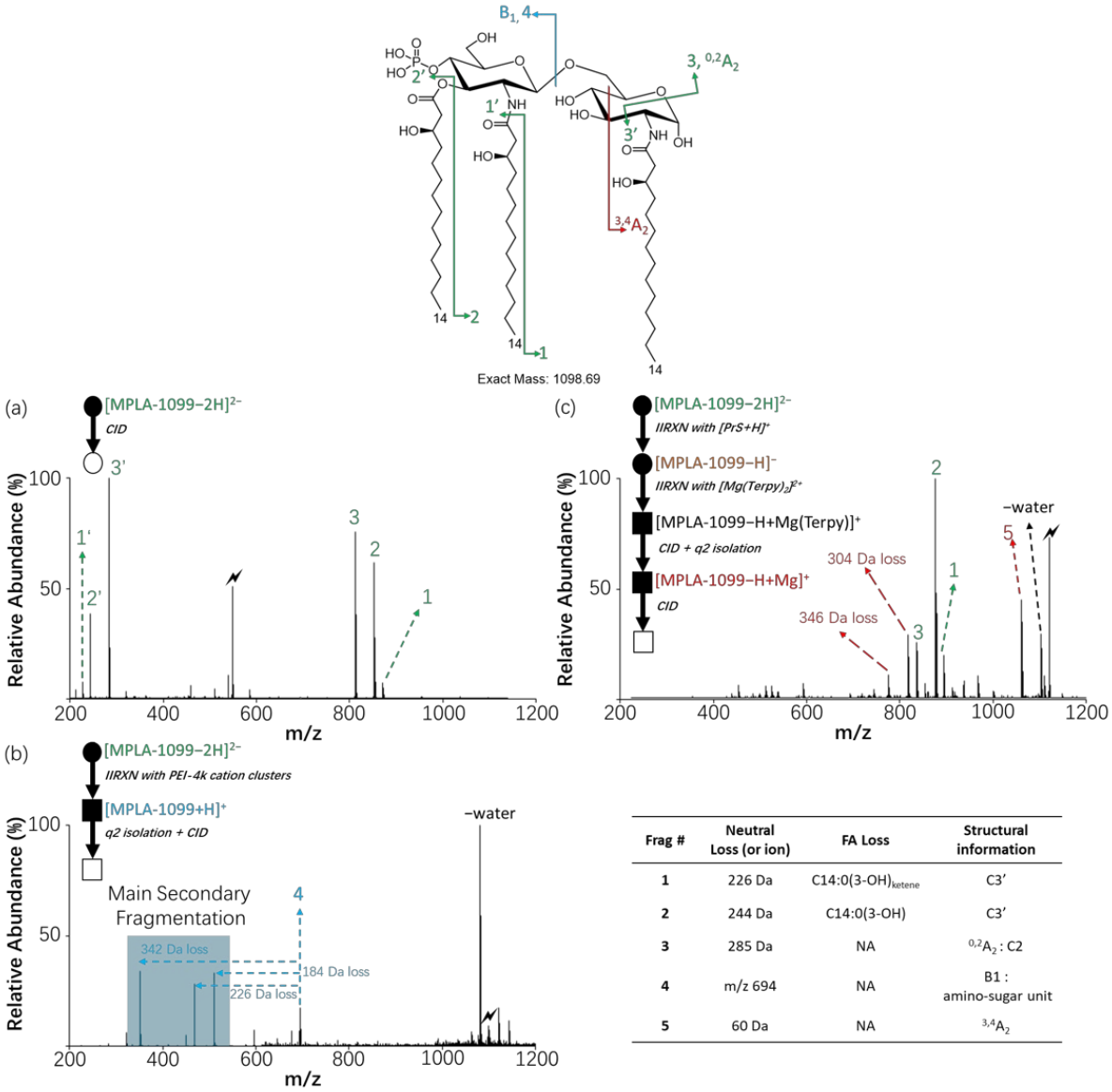

Frag #	Neutral Loss (or ion)	FA Loss	Structural information
1	226 Da	C14:0(3-OH)$_{ketene}$	C3′
2	244 Da	C14:0(3-OH)	C3′
3	285 Da	NA	$^{0,2}A_2$: C2
4	m/z 694	NA	B1 : amino-sugar unit
5	60 Da	NA	$^{3,4}A_2$

Figure 5. The CID mass spectra of different MPLA-1099 ions, (a) $[MPLA\text{-}1099{-}2H]^{2-}$, *m/z* 548.3 (b) $[MPLA\text{-}1099{+}H]^{+}$, *m/z* 1099.7, and (c) [MPLA-1099−H+Mg]+, *m/z* 1121.7

The analysis of DPLA via gas-phase chemistry. The complementary precursor ion-type approach was further extended to analyze diphosphorylated lipid A, by first investigating four different ion-types: $[DPLA-2H]^{2-}$, $[DPLA-H]^{-}$, $[DPLA+H]^{+}$, and $[DPLA-H+Mg]^{+}$. As with MPLAs, we summarize our observations before providing detailed explanations. Unlike MPLA, CID of $[DPLA-2H]^{2-}$ yields a single prominent fragment ion, while $[DPLA-H]^{-}$ provides a more detailed fatty acyl profile combined with glycosidic bond cleavage (Y1 ion). CID of $[DPLA+H]^{+}$ also leads to glycosidic bond cleavage, with the complementary ion (B1 ion) being dominant. These complementary B/Y ions allow for the structural elucidation of the sub-amino sugar unit. Lastly, the magnesium-transferred cation, $[DPLA-H+Mg]^{+}$, offers fatty acyl profile information, including additional fatty acyl information (C2' branch). DPLA extracts from the same *E. coli* F583 strain were again selected to test the method. Three major DPLA were profiled, including *m/z* 897.6 (2−), *m/z* 792.5 (2−), and *m/z* 679.5 (2−) (**Figure S8**). First, we subjected the ion at *m/z* 897.6 (2−) for further analysis, which is a DPLA with reported structures from previous reports (DPLA-1797).[26-27, 52] **Figure 6** shows the CID spectra from the four ion-types, including $[DPLA\text{-}1797-2H]^{2-}$, $[DPLA\text{-}1797-H]^{-}$, $[DPLA\text{-}1797+H]^{+}$, and $[DPLA\text{-}1797-H+Mg]^{+}$. **Figure 6a** shows the CID product ion spectrum of $[DPLA\text{-}1797-2H]^{2-}$ (*m/z* 897.6, 2−), which gives only a dominant 228 Da loss (m/z 783.6, 2−). This result suggests a potential C14:0 fatty acyl chain, but this information alone does not allow for the distinction between a branched C14:0 fatty acid on C3' or cleavages on C2 (aldehyde loss) or C3 positions based on the proposed structures. Next, CID of singly deprotonated DPLA shows more informative fragment ions compared to CID of doubly deprotonated DPLA. Upon CID of the singly deprotonated species, $[DPLA\text{-}1797-H]^{-}$, 98 Da loss (*m/z* 1698.3, phosphate loss, fragment 2), 200 Da loss (*m/z* 1596.1, C12:0 fatty acid, fragment 3), 228 Da loss (*m/z* 1568.0, C14:0 fatty acid), 244 Da loss (*m/z* 1552.0, C14:0(3-OH) fatty acyl, fragment 4), and 454 Da loss (*m/z* 1341.9, C14:0(3-O-C:14:0) were observed , as well as 324 Da loss (98 Da +226 Da loss), and 342 Da loss (98 Da + 244 Da loss) (**Figure 6b**.) The fatty acyl composition is

reflected from the above fragments. Also, the significant 244 Da loss suggests the loss of C14:0(3-OH) on the C3 position. We also observed 454 Da loss, which suggests the loss of whole fatty acyl unit on C3', but it is not as significant as the other fragments in the profile. Interestingly, a 1086 Da loss (*m/z* 710) stands out in the lower *m/z* region, which normally consists of low abundance secondary fragmentation, and it suggests the cleavage of the glycosidic bond for the Y_1 ion. Moreover, no significant signal from the complementary B_1 ion was observed in the spectrum, suggesting that the negative charge may be more stable on C1 phosphate group leading to the formation of Y_1 as well as C3 C14:0(3-OH) loss upon CID.

The CID of the singly protonated DPLA-1797, produced from a charge inversion reaction, was also performed (**Figure 6c**). Phosphate loss (98 Da loss, *m/z* 1700.2), 200 Da loss (*m/z* 1597.9, C12:0 fatty acid loss), and 711 Da loss (*m/z* 1086.8) were observed. In contrast to the CID of $[\text{DPLA-1797}-\text{H}]^-$ giving the Y_1 ion, CID of $[\text{DPLA-1797}+\text{H}]^+$ gives prominent B_1 ions, which is similar to singly protonated MPLA. We performed another round of CID on the ion at *m/z* 1086.8 (fragment 7), and a 200 Da loss (*m/z* 886.7) was observed, similar to the secondary fragments obtained in **Figure 6c**, and suggesting the C12:0 fatty acid to be on the first amino-sugar unit (data not shown).

Lastly, magnesium transferred DPLA cation, $[\text{DPLA-1797}-\text{H}+\text{Mg}]^+$ was produced by sequential ion/ion reaction and followed by ion trap CID. **Figure 6d** shows the fragment ion spectrum, including 98 Da loss (phosphate loss), 200 Da loss (C12:0 fatty acid loss), 228 Da loss (C14:0 fatty acid loss), 342 Da loss (98 Da + 244 Da loss), and 454 Da loss (C14:0(3-O-C14:0) fatty acyl unit loss) that are consistent with previous observations. However, fragment ions arising from 200 Da loss and 454 Da loss are more prominent in the profile, which may be associated with the magnesium coordinated site at the first amino-sugar unit (similar to MPLA), so the loss of C3' unit and C2' branched fatty acid are more prominent in the CID spectrum. Several other secondary fragmentations are also observed with high relative abundance, such as 552 Da loss (98 Da + 454 Da loss) and 654 Da loss (200 Da + 454 Da loss),

consistent with the fragmentation being closer to the favorable charged site.

In summary, the pieces of information that can be extracted from the various precursor ion types can be summarized as follows: (a) doubly deprotonated DPLA provides minimal information; (b) singly deprotonated DPLA offers C3 fatty acyl information combined with the Y_1 ion, allowing elucidation of the structure of the second amino-sugar unit; (c) singly protonated DPLA yields the B_1 ion and could potentially show fatty acyl chain loss in the first amino-sugar lipid conjugate unit, along with notable single phosphate loss; and (d) the magnesium-transferred DPLA cation delivers a detailed fragmentation profile of the fatty acyl chain composition at the C2' and potentially C3' positions. Consequently, we focused on $[DPLA\text{-}1797-H]^-$, $[DPLA\text{-}1797+H]^+$, and $[DPLA\text{-}1797-H+Mg]^+$ for structural analysis, as minimal information is obtained from $[DPLA\text{-}1797-2H]^{2-}$. Additionally, the DPLA-1587 structure, reported from engineered lipid A synthesis and analysis, was also considered.[27] Therefore, we verified our findings on this known DPLA (precursor m/z 792.5, 2−), and the results aligned with our findings from DPLA-1797 (**Figure S9**)

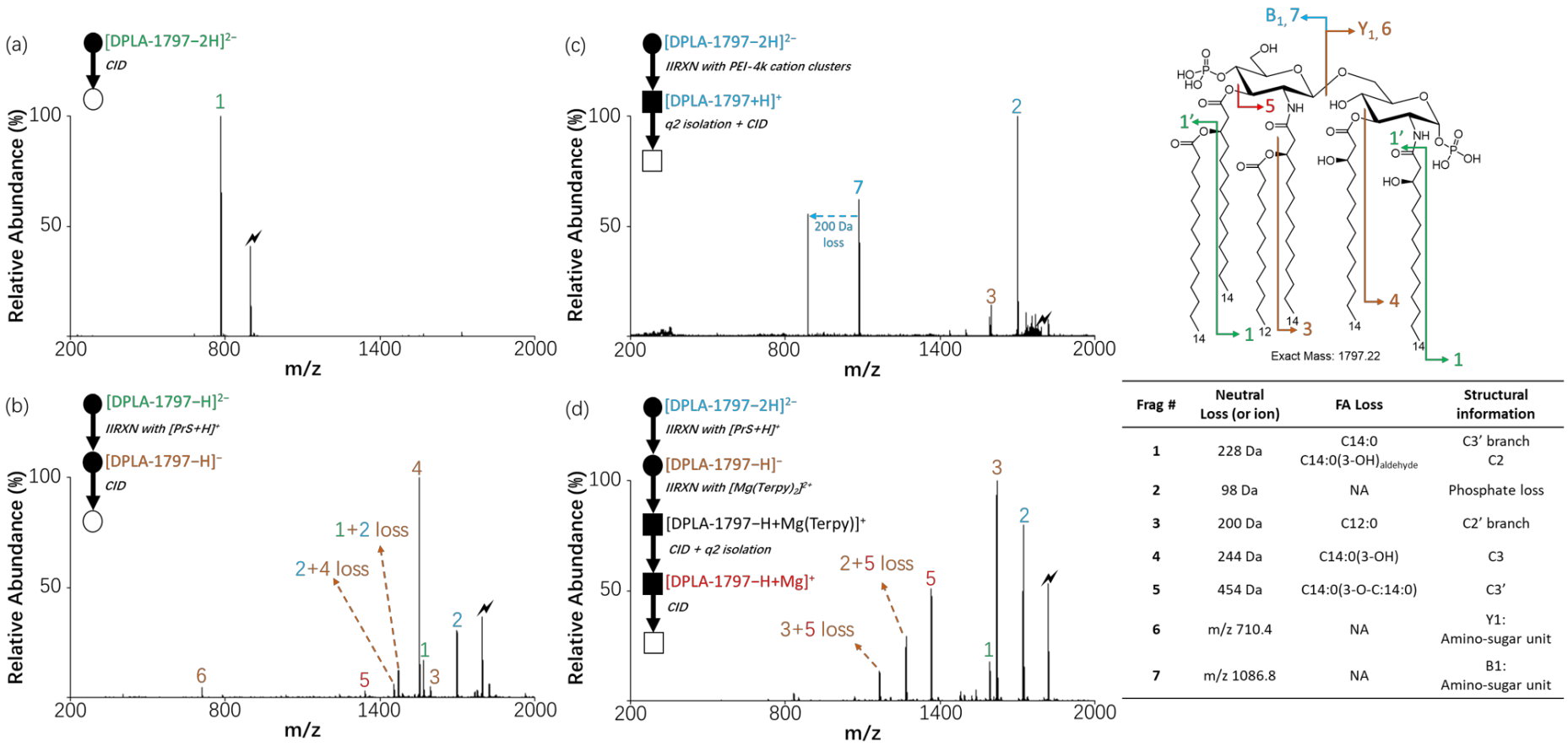

Frag #	Neutral Loss (or ion)	FA Loss	Structural information
1	228 Da	C14:0 $C14:0(3\text{-}OH)_{aldehyde}$	C3′ branch C2
2	98 Da	NA	Phosphate loss
3	200 Da	C12:0	C2′ branch
4	244 Da	C14:0(3-OH)	C3
5	454 Da	C14:0(3-O-C:14:0)	C3′
6	m/z 710.4	NA	Y1: Amino-sugar unit
7	m/z 1086.8	NA	B1: Amino-sugar unit

Figure 6. The CID mass spectra of different DPLA-1797 ions, (a) $[DPLA\text{-}1797{-}2H]^{2-}$, *m/z* 897.6 (b) $[DPLA\text{-}1797{-}H]^{-}$, *m/z* 1796.2, (c) $[DPLA\text{-}1797{+}H]^{+}$, *m/z* 1798.2, and (d) [DPLA-1797−H+Mg]+, *m/z* 1820.2.

Structural elucidation of unknown DPLA in E. coli F583 extract. The third dominant lipid A that we profiled in the *E. coli* extract, *m/z* 679.4 (2−), which is denoted as DPLA-1361 herein, was subjected to the structural analysis. A lipid A of the mass of DPLA-1361 has been reported in the engineered lipid A literature,[27] but the data we obtained from our strategy suggested a different structure. Therefore, we treated it as a new unknown lipid A. Note that the *E. coli* strain used in this work differs from that of the literature work cited above, so enzymatic reactions may be different between different strains, leading to different structures. $[DPLA\text{-}1361-H]^-$, $[DPLA\text{-}1361+H]^+$, and $[DPLA\text{-}1361-H+Mg]^+$ were individually generated via the various gas-phase ion/ion reactions, following by ion trap CID for structural elucidation (**Figure 7**). First, CID of $[DPLA\text{-}1361-H]^-$ (*m/z* 1359.8) leads to a prominent 244 Da loss (*m/z* 1115.8, fragment 1) suggesting a C14:0(3-OH) fatty acyl chain on the C3 position, and the Y_1 ion, *m/z* 710.4 (fragment 3). Similar to the results observed for DPLA-1797, a 98 Da loss (*m/z* 1261.9, fragment 2), a 324 Da loss (98 Da +226 Da loss), and a 342 Da loss (98 Da + 244 Da loss) are also observed, suggesting a similar Y_1 ion structure to DPLA-1797 (**Figure 7a**). However, the absence of 228 Da and 454 Da losses indicates the potential absence of a C14:0 fatty acid branch on the C3' position.

Next, CID of $[DPLA\text{-}1361+H]^+$ (*m/z* 1361.7) shows a dominant 98 Da loss, with B_1 ion information, *m/z* 650.3 (711 Da loss, fragment 4), suggesting a smaller amino sugar-lipid conjugate than the Y_1 ion. A secondary fragmented ion is also observed with additional 200 Da loss to the B_1 ion. We also tried to verify the secondary fragmentation by another round CID on B_1 ion, and the result agree with **Figure 7b** (data not shown). The 200 Da loss suggests that a C12:0 fatty acid is on the B_1 structure. An additional 116 Da loss is also observed as a secondary fragmentation to B_1 ion, which may be the combination of the loss of water and phosphate (18 + 98 Da.)

Finally, CID of $[DPLA\text{-}1361-H+Mg]^+$ (*m/z* 1383.8) shows distinct fragment profiles comparing to DPLA-1797, where only prominent 98 Da loss and 200 Da loss (*m/z* 1183.6,

fragment 5) are observed (**Figure 7c**.) This result with the 116 Da loss from the CID of B_1 ion indicates no C3' fatty acyl component is on the structure (since water loss is not observed in other DPLAs), and the 200 Da is the C12:0 fatty acid branch at C2' position. Therefore, we are able to proposed a single structure of this unknown lipid A.

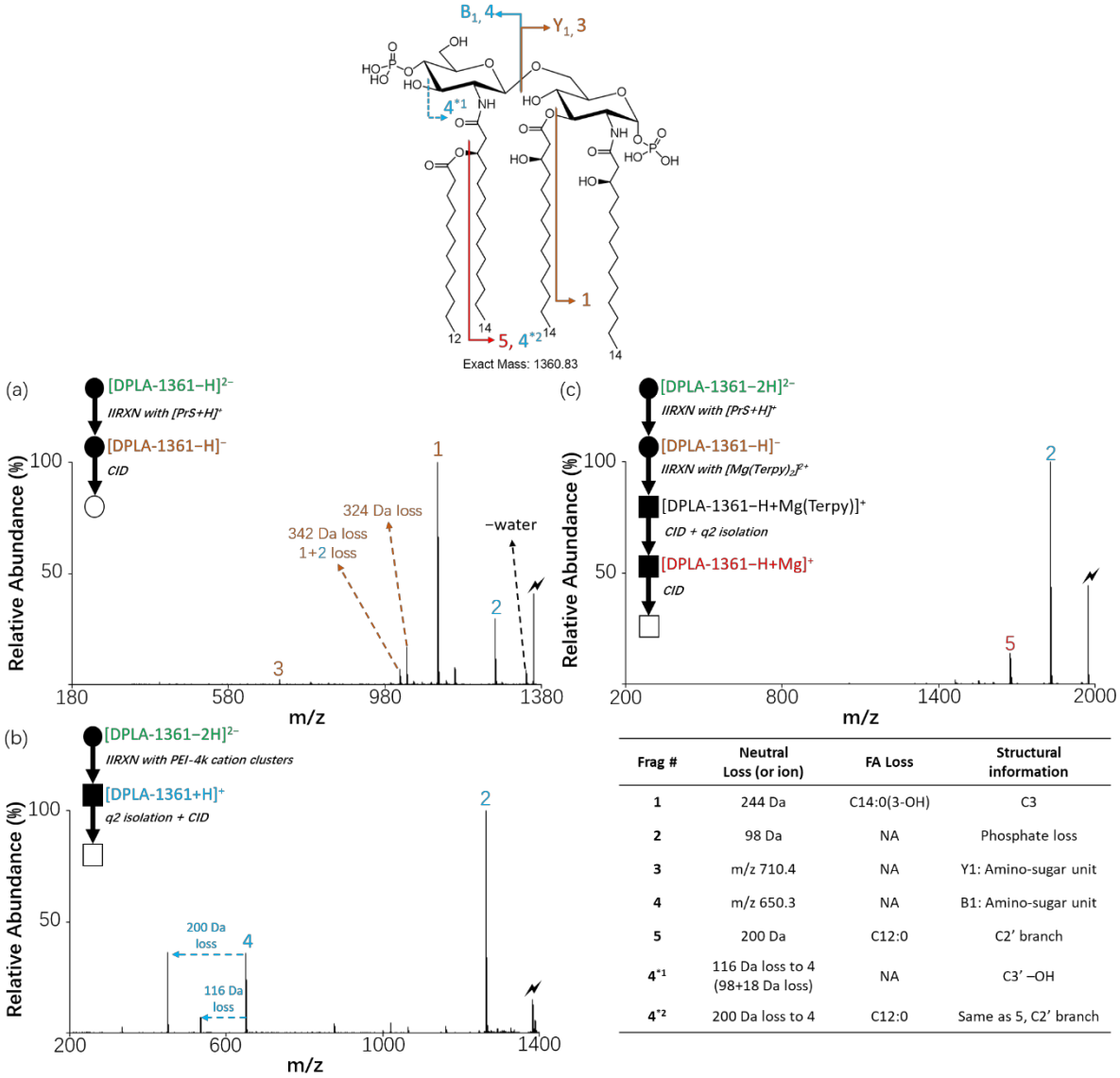

Frag #	Neutral Loss (or ion)	FA Loss	Structural information
1	244 Da	C14:0(3-OH)	C3
2	98 Da	NA	Phosphate loss
3	m/z 710.4	NA	Y1: Amino-sugar unit
4	m/z 650.3	NA	B1: Amino-sugar unit
5	200 Da	C12:0	C2′ branch
4^{*1}	116 Da loss to 4 (98+18 Da loss)	NA	C3′ –OH
4^{*2}	200 Da loss to 4	C12:0	Same as 5, C2′ branch

Figure 7. The CID mass spectra of different DPLA-1361 ions, (a) [MPLA-1361−H]$^-$, *m/z* 1359.8 (b) [MPLA-1361+H]$^+$, *m/z* 1361.8, and (c) [MPLA-1361−H+Mg]+, *m/z* 1383.8

Scheme 1 outlines our strategy, detailing the workflow from sample preparation to the use of various gas-phase ion/ion reactions for generating different ion-types and the structural information each ion-type provides for MPLA and DPLA species. While targeted ion types for complementary structural information can be prepared using various condensed phase methods, gas-phase ion/ion reactions provide a purely online approach with short reaction times (10-50 ms) and flexibility (easy switching of reaction reagents) to produce diverse ion-types for analysis. We believe this workflow not only streamlines the structural analysis of lipid A but also has the potential to increase throughput in profiling lipid A species using online gas-phase ion chemistry.

Conclusion

Characterizing lipid A structures is challenging due to their complexity. Researchers have proposed various strategies, with the most common approach being the acquisition of complementary structural information from different ion-types and through diverse dissociation techniques. In this study, we advanced this approach by employing gas-phase ion/ion reactions to generate targeted ion-types for subsequent ion-trap CID, thus obtaining complementary structural information from a given lipid A. Additionally, we performed a condensed phase pH adjustment using ammonium hydroxide to enhance the signal of the doubly deprotonated precursor lipid A anion via the ESI process. This simple step led to a roughly 15-fold improvement in precursor ion signal. Several ion/ion reactions were employed to produce targeted ion types for both MPLA and DPLA. Our findings indicate that using ion-trap CID on doubly deprotonated MPLA ($[MPLA-2H]^{2-}$), protonated MPLA ($[MPLA+H]^{+}$), and magnesium-transferred MPLA cation ($[MPLA-H+Mg]^{+}$) provides comprehensive fragmentation information, enabling full profiling of MPLA structures. This strategy, based on known synthetic MPLA-PHAD and two other MPLAs (MPLA-1507 and MPLA-1281) from the *E. coli* F583 strain, was validated by profiling the unknown MPLA-1098 structure.

Similarly, deprotonated DPLA ($[DPLA-H]^-$), protonated DPLA ($[DPLA+H]^+$), and magnesium-transferred DPLA cation ($[DPLA-H+Mg]^+$) offered complementary structural information to fully profile DPLA structures. We established the strategy using two known DPLAs (DPLA-1797 and DPLA-1361) from the *E. coli* F583 strain and validated it with an unknown DPLA-1361. In summary, the combined use of condensed phase sample preparation and online gas-phase ion/ion reactions for generating targeted ion types, followed by ion-trap CID, provides a comprehensive approach for lipid A analysis, as detailed in Scheme 1. However, some form of prior separation may be required to account for the existence of isomeric lipid A structures. In conclusion, utilizing online gas-phase reactions allows us to easily modify precursor lipid A into targeted ion types for obtaining structural information.

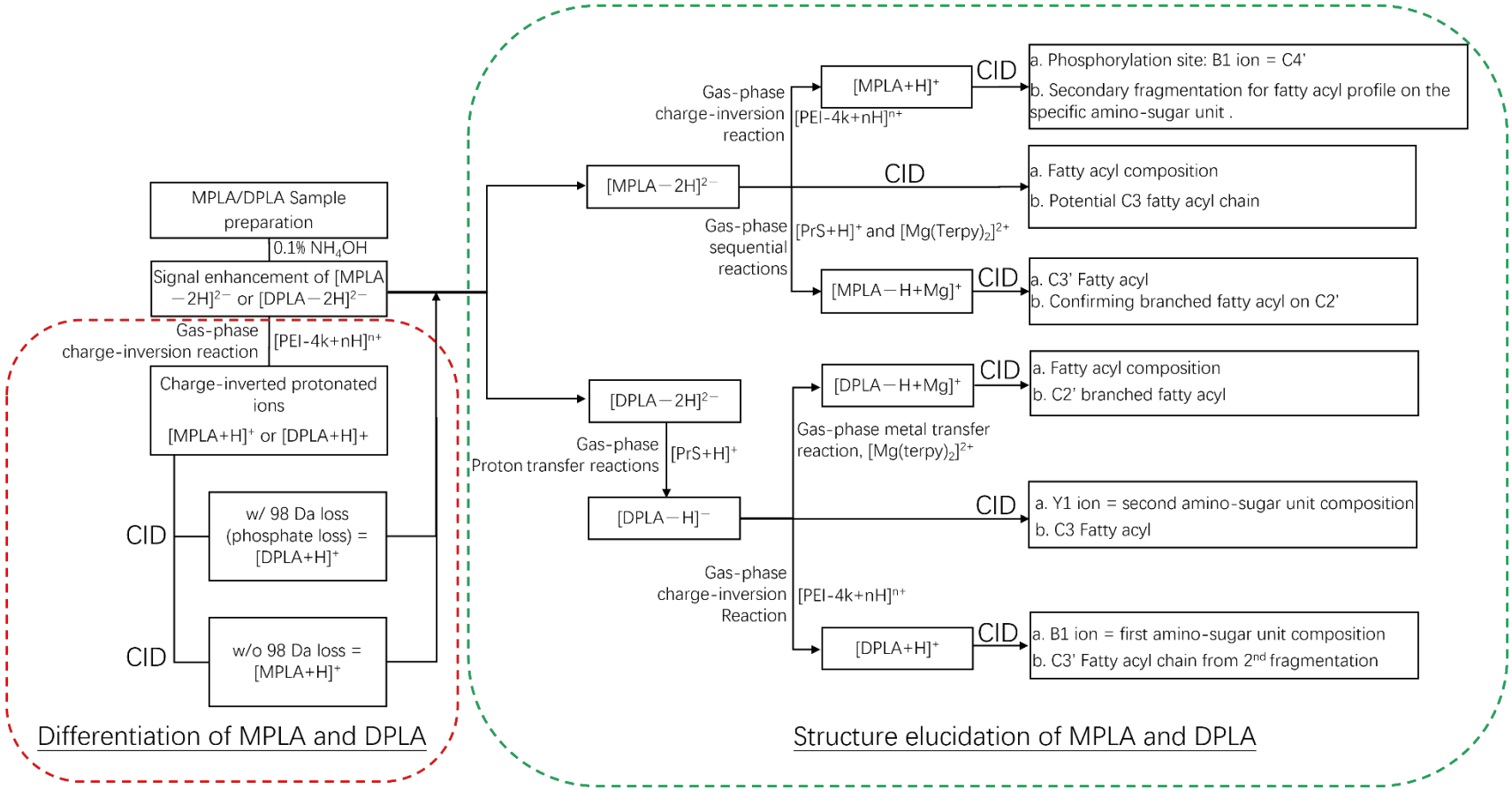

Scheme 1. The workflow for utilizing gas-phase ion reactions for in-depth structural elucidation of lipid A species, including MPLA and DPLA.

ACKNOWLEDGEMENTS

This research was supported by the National Science Foundation CHE-2304386. The authors would like to acknowledge Dr Liangxuan Fu helpful discussions. The authors also acknowledge SCIEX, and particularly Mr. Frank Londry, for modifying the instruments to enable the ion/ion reaction experiments.

DATA AVAILABILITY STATEMENT

The data that support the findings of this study are available from the corresponding author upon reasonable request.

ORCID

Hsi-Chun Chao - orcid.org/0000-0003-1774-4877; Email: hcchao@illinois.edu

Scott A. McLuckey - orcid.org/0000-0002-1648-5570; Email: mcluckey@purdue.edu

Supporting Information

Additional supporting information can be found online in the Supporting Information section at the end of this article.

AUTHOR INFORMATION

Corresponding Author

Scott A. McLuckey - Department of Chemistry, Purdue University, West Lafayette, Indiana 47907-2084, United States, orcid.org/0000-0002-1648-5570; Email: mcluckey@purdue.edu

Authors

Hsi-Chun Chao - Department of Chemistry, Purdue University, West Lafayette, Indiana 47907-2084, United States, $current institute: Beckman Institute for Advanced Science and Technology, University of Illinois Urbana-Champaign, Illinois, 61801; orcid.org/0000-0003-1774-4877; Email: hcchao@illinois.edu

Credit Author Statement

Hsi-Chun Chao: Investigation, data curation, methodology, visualization, writing - original draft preparation. **Scott A. McLuckey:** Methodology, resources, supervision, visualization, writing – review and editing.

Notes

The authors declare no competing financial interests.

References

1. Fahy, E.; Sud, M.; Cotter, D.; Subramaniam, S., LIPID MAPS online tools for lipid research. *Nucleic Acids Res.* **2007,** *35* (Web Server issue), W606-W612.

2. Fahy, E.; Subramaniam, S.; Brown, H. A.; Glass, C. K.; Merrill, A. H., Jr.; Murphy, R. C.; Raetz, C. R. H.; Russell, D. W.; Seyama, Y.; Shaw, W.; Shimizu, T.; Spener, F.; van Meer, G.; VanNieuwenhze, M. S.; White, S. H.; Witztum, J. L.; Dennis, E. A., A comprehensive classification system for lipids. *J. Lipid Res.* **2005,** *46* (5), 839-861.
3. Wang, X.; Quinn, P. J., Lipopolysaccharide: Biosynthetic pathway and structure modification. *Prog. Lipid Res.* **2010,** *49* (2), 97-107.
4. Steimle, A.; Autenrieth, I. B.; Frick, J.-S., Structure and function: Lipid A modifications in commensals and pathogens. *Int. J. Me. Microbiol.* **2016,** *306* (5), 290-301.
5. Rietschel, E. T.; Kirikae, T.; Schade, F. U.; Mamat, U.; Schmidt, G.; Loppnow, H.; Ulmer, A. J.; Zähringer, U.; Seydel, U.; Di Padova, F.; Schreier, M.; Brade, H., Bacterial endotoxin: molecular relationships of structure to activity and function. *FASEB J.* **1994,** *8* (2), 217-225.
6. Kilár, A.; Dörnyei, Á.; Kocsis, B., Structural characterization of bacterial lipopolysaccharides with mass spectrometry and on- and off-line separation techniques. *Mass Spectrom. Rev.* **2013,** *32* (2), 90-117.
7. Buré, C.; Le Sénéchal, C.; Macias, L.; Tokarski, C.; Vilain, S.; Brodbelt, J. S., Characterization of Isomers of Lipid A from Pseudomonas aeruginosa PAO1 by Liquid Chromatography with Tandem Mass Spectrometry with Higher-Energy Collisional Dissociation and Ultraviolet Photodissociation. *Anal. Chem.* **2021,** *93* (9), 4255-4262.
8. Rietschel, E. T.; Sidorczyk, Z.; Zähringer, U.; Wollenweber, H.-W.; Lüderitz, O., Analysis of the Primary Structure of Lipid A. In *Bacterial Lipopolysaccharides*, ACS: 1983; Vol. 231, pp 195-218.
9. Nurminen, M.; Rietschel, E. T.; Brade, H., Chemical characterization of Chlamydia trachomatis lipopolysaccharide. *Infec. Immu.* **1985,** *48* (2), 573-575.
10. Imoto, M.; Kusumoto, S.; Shiba, T.; Naoki, H.; Iwashita, T.; Rietschel, E. T.; Wollenweber, H. W.; Galanos, C.; Lüderitz, O., Chemical structure of E. Coli Lipid A: Linkage site of acyl groups in the disaccharide backbone. *Tetrahedron Lett.* **1983,** *24* (37), 4017-4020.
11. Gibson, B. W.; Engstrom, J. J.; John, C. M.; Hines, W.; Falick, A. M., Characterization of bacterial lipooligosaccharides by delayed extraction matrix-assisted laser desorption ionization time-of-flight mass spectrometry. *J. Am. Soc. Mass Spectrom.* **1997,** *8* (6), 645-658.
12. Qureshi, N.; Kaltashov, I.; Walker, K.; Doroshenko, V.; Cotter, R. J.; Takayama, K.; Sievert, T. R.; Rice, P. A.; Lin, J.-S. L.; Golenbock, D. T., Structure of the Monophosphoryl Lipid A Moiety Obtained from the Lipopolysaccharide of *Chlamydia trachomatis*. *J. Biol. Chem.* **1997,** *272* (16), 10594-10600.
13. Kaltashov, I. A.; Doroshenko, V.; Cotter, R. J.; Takayama, K.; Qureshi, N., Confirmation of the Structure of Lipid A Derived from the Lipopolysaccharide of Rhodobacter sphaeroides

by a Combination of MALDI, LSIMS, and Tandem Mass Spectrometry. *Anal. Chem.* **1997,** *69* (13), 2317-2322.
14. Zhou, P.; Altman, E.; Perry, M. B.; Li, J., Study of Matrix Additives for Sensitive Analysis of Lipid A by Matrix-Assisted Laser Desorption Ionization Mass Spectrometry. *Appl. Environ. Microbiol.* **2010,** *76* (11), 3437-3443.
15. Murphy, R. C.; Raetz, C. R. H.; Reynolds, C. M.; Barkley, R. M., Mass spectrometry advances in lipidomica: collision-induced decomposition of Kdo2–lipid A. *Prostaglandins Other Lipid Mediat.* **2005,** *77* (1), 131-140.
16. Sturiale, L.; Palmigiano, A.; Silipo, A.; Knirel, Y. A.; Anisimov, A. P.; Lanzetta, R.; Parrilli, M.; Molinaro, A.; Garozzo, D., Reflectron MALDI TOF and MALDI TOF/TOF mass spectrometry reveal novel structural details of native lipooligosaccharides. *J. Mass. Spectrom.* **2011,** *46* (11), 1135-1142.
17. Griffiths, R. L.; Bunch, J., A survey of useful salt additives in matrix-assisted laser desorption/ionization mass spectrometry and tandem mass spectrometry of lipids: introducing nitrates for improved analysis. *Rapid Commun. Mass Spectrom.* **2012,** *26* (13), 1557-1566.
18. Park, H.-G.; Sathiyanarayanan, G.; Hwang, C.-H.; Ann, D.-H.; Kim, J.-H.; Bang, G.; Jang, K.-S.; Ryu, H. W.; Lee, Y. K.; Yang, Y.-H.; Kim, Y.-G., Chemical Structure of the Lipid A component of Pseudomonas sp. strain PAMC 28618 from Thawing Permafrost in Relation to Pathogenicity. *Sci. Rep.* **2017,** *7* (1), 2168.
19. Chan, S.; Reinhold, V. N., Detailed Structural Characterization of Lipid A: Electrospray Ionization Coupled with Tandem Mass-Spectrometry. *Anal. Biochem.* **1994,** *218* (1), 63-73.
20. Silipo, A.; De Castro, C.; Lanzetta, R.; Molinaro, A.; Parrilli, M.; Vago, G.; Sturiale, L.; Messina, A.; Garozzo, D., Structural characterizations of lipids A by MS/MS of doubly charged ions on a hybrid linear ion trap/orbitrap mass spectrometer. *J. Mass Spectrom.* **2008,** *43* (4), 478-484.
21. Wang, Z.; Li, J.; Altman, E., Structural characterization of the lipid A region of Aeromonas salmonicida subsp. salmonicida lipopolysaccharide. *Carbohydr. Res.* **2006,** *341* (17), 2816-2825.
22. Sándor, V.; Kilár, A.; Kilár, F.; Kocsis, B.; Dörnyei, Á., Characterization of complex, heterogeneous lipid A samples using HPLC-MS/MS technique III. Positive-ion mode tandem mass spectrometry to reveal phosphorylation and acylation patterns of lipid A. *J. Mass. Spectrom.* **2018,** *53* (2), 146-161.
23. Tawab, A.; Akbar, N.; Hasssan, M.; Habib, F.; Ali, A.; Rahman, M.; Jabbar, A.; Rauf, W.; Iqbal, M., Mass spectrometric analysis of lipid A obtained from the lipopolysaccharide of Pasteurella multocida. *RSC Advances* **2020,** *10* (51), 30917-30933.
24. Jones, J. W.; Shaffer, S. A.; Ernst, R. K.; Goodlett, D. R.; Tureček, F., Determination of pyrophosphorylated forms of lipid A in Gram-negative bacteria using a multivaried mass spectrometric approach. *Proc. Natl. Acad. Sci. U.S.A.* **2008,** *105* (35), 12742-12747.

25. Jones, J. W.; Cohen, I. E.; Turečček, F.; Goodlett, D. R.; Ernst, R. K., Comprehensive Structure Characterization of Lipid A Extracted from Yersinia pestis for Determination of its Phosphorylation Configuration. *J. Am. Soc. Mass. Spectrom.* **2010,** *21* (5), 785-799.
26. Madsen, J. A.; Cullen, T. W.; Trent, M. S.; Brodbelt, J. S., IR and UV Photodissociation as Analytical Tools for Characterizing Lipid A Structures. *Anal. Chem.* **2011,** *83* (13), 5107-5113.
27. O'Brien, J. P.; Needham, B. D.; Henderson, J. C.; Nowicki, E. M.; Trent, M. S.; Brodbelt, J. S., 193 nm Ultraviolet Photodissociation Mass Spectrometry for the Structural Elucidation of Lipid A Compounds in Complex Mixtures. *Anal. Chem.* **2014,** *86* (4), 2138-2145.
28. Brodbelt, J. S.; Morrison, L. J.; Santos, I., Ultraviolet Photodissociation Mass Spectrometry for Analysis of Biological Molecules. *Chem. Rev.* **2020,** *120* (7), 3328-3380.
29. McLuckey, S. A.; Mentinova, M., Ion/Neutral, Ion/Electron, Ion/Photon, and Ion/Ion Interactions in Tandem Mass Spectrometry: Do We Need Them All? Are They Enough? *J. Am. Soc. Mass. Spectrom.* **2011,** *22* (1), 3-12.
30. Aissa, I.; Dörnyei, Á.; Sándor, V.; Kilár, A., Complete Structural Elucidation of Monophosphorylated Lipid A by CID Fragmentation of Protonated Molecule and Singly Charged Sodiated Adducts. *J. Am. Soc. Mass. Spectrom.* **2023,** *34* (1), 92-100.
31. Sándor, V.; Berkics, B. V.; Kilár, A.; Kocsis, B.; Kilár, F.; Dörnyei, Á., NACE–ESI-MS/MS method for separation and characterization of phosphorylation and acylation isomers of lipid A. *Electrophoresis* **2020,** *41* (13-14), 1178-1188.
32. Sforza, S.; Silipo, A.; Molinaro, A.; Marchelli, R.; Parrilli, M.; Lanzetta, R., Determination of fatty acid positions in native lipid A by positive and negative electrospray ionization mass spectrometry. *J. Mass Spectrom.* **2004,** *39* (4), 378-383.
33. Patil, A. A.; Descanzo, M. J. N.; Dhisale, V. B.; Peng, W.-P., MALDI sample preparation methods: A mini review. *Int. J. Mass spectrom.* **2024,** *498*, 117219.
34. Bonfiglio, R.; King, R. C.; Olah, T. V.; Merkle, K., The effects of sample preparation methods on the variability of the electrospray ionization response for model drug compounds. *Rapid Commun. Mass Spectrom.* **1999,** *13* (12), 1175-1185.
35. Foreman, D. J.; McLuckey, S. A., Recent Developments in Gas-Phase Ion/Ion Reactions for Analytical Mass Spectrometry. *Anal. Chem.* **2020,** *92* (1), 252-266.
36. Randolph, C. E.; Foreman, D. J.; Betancourt, S. K.; Blanksby, S. J.; McLuckey, S. A., Gas-Phase Ion/Ion Reactions Involving Tris-Phenanthroline Alkaline Earth Metal Complexes as Charge Inversion Reagents for the Identification of Fatty Acids. *Anal. Chem.* **2018,** *90* (21), 12861-12869.
37. Franklin, E. T.; Betancourt, S. K.; Randolph, C. E.; McLuckey, S. A.; Xia, Y., In-depth structural characterization of phospholipids by pairing solution photochemical reaction with charge inversion ion/ion chemistry. *Anal. Bioanal. Chem.* **2019,** *411* (19), 4739-4749.

38. Randolph, C. E.; Blanksby, S. J.; McLuckey, S. A., Toward Complete Structure Elucidation of Glycerophospholipids in the Gas Phase through Charge Inversion Ion/Ion Chemistry. *Anal. Chem.* **2020,** *92* (1), 1219-1227.
39. Randolph, C. E.; Shenault, D. S. M.; Blanksby, S. J.; McLuckey, S. A., Structural Elucidation of Ether Glycerophospholipids Using Gas-Phase Ion/Ion Charge Inversion Chemistry. *J. Am. Soc. Mass. Spectrom.* **2020,** *31* (5), 1093-1103.
40. Randolph, C. E.; Fabijanczuk, K. C.; Blanksby, S. J.; McLuckey, S. A., Proton Transfer Reactions for the Gas-Phase Separation, Concentration, and Identification of Cardiolipins. *Anal. Chem.* **2020,** *92* (15), 10847-10855.
41. Randolph, C. E.; Shenault, D. S. M.; Blanksby, S. J.; McLuckey, S. A., Localization of Carbon–Carbon Double Bond and Cyclopropane Sites in Cardiolipins via Gas-Phase Charge Inversion Reactions. *J. Am. Soc. Mass. Spectrom.* **2021,** *32* (2), 455-464.
42. Chao, H.-C.; McLuckey, S. A., Differentiation and Quantification of Diastereomeric Pairs of Glycosphingolipids Using Gas-Phase Ion Chemistry. *Anal. Chem.* **2020,** *92* (19), 13387-13395.
43. Chao, H.-C.; McLuckey, S. A., In-Depth Structural Characterization and Quantification of Cerebrosides and Glycosphingosines with Gas-Phase Ion Chemistry. *Anal. Chem.* **2021,** *93* (19), 7332-7340.
44. Fabijanczuk, K. C.; Chao, H.-C.; Fischer, J. L.; McLuckey, S. A., Structural elucidation and isomeric differentiation/quantitation of monophosphorylated phosphoinositides using gas-phase ion/ion reactions and dissociation kinetics. *Analyst* **2022,** *147* (22), 5000-5010.
45. Chao, H.-C.; McLuckey, S. A., Manipulation of Ion Types via Gas-Phase Ion/Ion Chemistry for the Structural Characterization of the Glycan Moiety on Gangliosides. *Anal. Chem.* **2021,** *93* (47), 15752-15760.
46. Bhanot, J. S.; Fabijanczuk, K. C.; Abdillahi, A. M.; Chao, H.-C.; Pizzala, N. J.; Londry, F. A.; Dziekonski, E. T.; Hager, J. W.; McLuckey, S. A., Adaptation and operation of a quadrupole/time-of-flight tandem mass spectrometer for high mass ion/ion reaction studies. *Int. J. Mass spectrom.* **2022,** *478*, 116874.
47. Xia, Y.; Liang, X.; McLuckey, S. A., Pulsed Dual Electrospray Ionization for Ion/Ion Reactions. *J. Am. Soc. Mass. Spectrom.* **2005,** *16* (11), 1750-1756.
48. McLuckey, S. A.; Reid, G. E.; Wells, J. M., Ion Parking during Ion/Ion Reactions in Electrodynamic Ion Traps. *Anal. Chem.* **2002,** *74* (2), 336-346.
49. Chao, H.-C.; Shih, M.; McLuckey, S. A., Generation of Multiply Charged Protein Anions from Multiply Charged Protein Cations via Gas-Phase Ion/Ion Reactions. *J. Am. Soc. Mass. Spectrom.* **2020,** *31* (7), 1509-1517.
50. McLuckey, S. A.; Goeringer, D. E.; Glish, G. L., Selective ion isolation/rejection over a broad mass range in the quadrupole ion trap. *J. Am. Soc. Mass. Spectrom.* **1991,** *2* (1), 11-21.
51. Valvano, M. A., Chapter 4 - Genetics and Biosynthesis of Lipopolysaccharide. In

Molecular Medical Microbiology (Second Edition), Tang, Y.-W.; Sussman, M.; Liu, D.; Poxton, I.; Schwartzman, J., Eds. Academic Press: Boston, 2015; pp 55-89.
52. Yang, H.; Chandler, C. E.; Jackson, S. N.; Woods, A. S.; Goodlett, D. R.; Ernst, R. K.; Scott, A. J., On-Tissue Derivatization of Lipopolysaccharide for Detection of Lipid A Using MALDI-MSI. *Anal. Chem.* **2020,** *92* (20), 13667-13671.